# Photonic Crystal Fibers - Viscous Behaviour of Silica Tubes During Collapsing and Hollow Fiber Drawing.

J. Kirchhof, K. Gerth, J. Kobelke, and K. Schuster
*Institut für Physikalische Hochtechnologie Jena*
*P.O.B. 100 239, D-07702 Jena, Germany*

As a contribution to the technology of „photonic crystal fibers“, an elementary model is developed for the description of collapsing and drawing of capillaries from preform tubes. The results of calculations are compared with experiments and the effect of surface tension and pressure differences on the capillary dimension is clarified.

## 1. Introduction

Silica based "photonic crystal fibers" are a novel type of lightguides with peculiar properties attractive for a wide range of optical applications[1]. These fibers consist of a more or less regular arrangement of air holes with specified diameter and spacing around a glassy or hollow core. Normally, they are made by collapsing and drawing of capillaries with different diameters in several preparation steps. Till now, the fabrication technique is fairly immature and developed on an empirical approach.

As a contribution to the technology of "photonic crystal fibers", we consider here the combined drawing and collapsing of a single glass capillary on the basis of an elementary model. Strictly spoken, we neglect the radial dependence of the axial flow velocity. This approach, which is often used in the consideration of solid fiber drawing [see e.g.[2,3]], cannot represent all subtle details of the real process. It is, however, very helpful for the basic understanding and the estimation of the effect of pressure differences between the inner and outer atmosphere of the hollow tube, which will be the central aim of our investigations here. In the treatment of capillary drawing, little attention was paid to this effect up to now[4,5,6].

## 2. The viscous flow mechanics during collapsing and fiber drawing

### 2.1 The homogeneous flow behaviour of a hollow cylinder

The homogeneous elongation or compression of a cylinder is one of the simplest examples in the theory of the viscous flux, with different applications, e.g. the viscosity determination by fiber elongation, but also in the theory of sintering porous glass bodies[7].Consider a hollow cylinder with outer radius $r_a$, inner radius $r_i$, and length $\lambda$. Under the influence of outer forces the dimensions of this tube are allowed to change by viscous flow, however preserving the cylindrical shape. This means we have to do with radial and axial components of the velocity **v** in the form $v_\varrho(\varrho)$ and $v_z(z)$, where $\varrho$, z are the cylindrical coordinates suitable for solving the problem. Taking the tube material as an incompressible Newtonian fluid, the flow can be described by the Navier-Stokes equations in Stokes flow approximation (neglection of acceleration forces)[8].

$$\eta \, \mathrm{rot} \, \mathrm{rot} \, \mathbf{v} + \mathrm{grad} \, p = 0 \qquad (1)$$

$$\mathrm{div} \, \mathbf{v} = 0 \qquad (2)$$

$\eta$ and p are viscosity and isotropic pressure in the medium, respectively.
From the incompressibility (2), the equations of the velocity components follow immediately .

$$v_z = K_1 z \qquad (3)$$

$$v_\varrho = - K_1(\varrho/2) + K_2(1/\varrho) \qquad (4)$$

With (3) and(4), the frictional pressure components $p_{\varrho\varrho} = -2\eta \, \partial v_\varrho/\partial\varrho$ and $p_{zz} = -2\eta \, \partial v_z/\partial z$ can be calculated in dependence on $K_1$ and $K_2$, and p becomes constant as a consequence of (1).

On the surfaces of the cylinder, the normal components $p + p_{ii}$ equilibrate with the outer pressures hown in Fig.1.

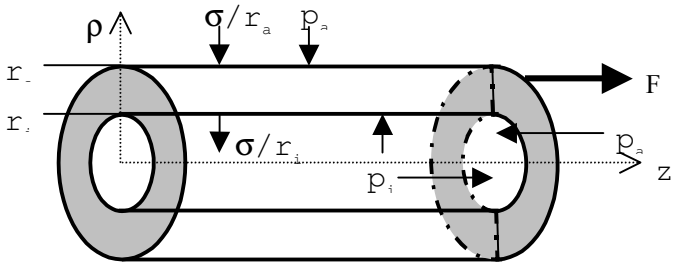


Fig. 1: Scheme of outside forces acting on the hollow cylinder

$p_a$ and $p_i$ are the atmospheric pressures outside and inside of the (closed) tube, $\sigma$ is the surface tension of the tube material, and F is a tensional force acting on the front face of the cylinder. Note that here the contribution of the front face to the surface energy of the cylinder is neglegted. This means the considerations are justified for a long cylinder with $\lambda >> r_a - r_i$ or (which agrees with our following applications) for a volume element of a continuos cylinder where the front surfaces are not free. After some arithmetics, the differential equations which govern the temporal change of tube radii and length are obtained.

$$d\lambda/dt = K_1\lambda \tag{5}$$

$$dr_a/dt = - K_1(r_a/2) + K_2(1/r_a) \tag{6}$$

$$dr_i/dt = - K_1(r_i/2) + K_2(1/r_i) \tag{7}$$

$$K_1 = \frac{1}{3\eta\,(r_a^2 - r_i^2)}\,(F/\pi - \sigma[r_a + r_i]) \tag{8}$$

$$K_2 = \frac{r_a^2\, r_i^2}{2\eta\,(r_a^2 - r_i^2)}\,(\Delta p - \sigma[r_a^{-1} + r_i^{-1}]) \tag{9}$$

The term $K_1$ accounts for the „drawing“, i.e. the proportional variation of $r_a$ and $r_i$, and the term $K_2$ describes the „collapsing“ (including also a „blowing up“) of the tube.

#### 2.2 Application to the tube collapse

If the drawing tension is set to zero, we have the case of a "free collapse" of the tube where the tube length is decreased by the surface tension alone. More important than the "free collapse", which is difficult to realize, is the case where the length of the tube remains constant, the usual collapsing of a tube mounted in a glass working lathe. Then, $K_1$ is constrained to be zero which means that a certain force $F = \pi\sigma(r_a + r_i)$ is generated in the cylinder faces. It is advantageous to transform the time variable t into a dimensionless coordinate $\tau_c$ acc. to

$$d\tau_c = \frac{\sigma}{2\eta\,(r_a^2 - r_i^2)^{1/2}}\,dt \tag{10}$$

with

$$K_{2c} = \frac{r_a^2\, r_i^2}{\sigma\,(r_a^2 - r_i^2)^{1/2}}\,(\Delta p - \sigma[r_a^{-1} + r_i^{-1}]) \tag{11}$$

Replacing dt by $d\tau_c$, $K_1$ by $K_{1c} = 0$, and $K_2$ by $K_{2c}$ adapts the equations (5 .. 9) to the collapse case. This leads to the same equations which were derived earlier for the case of the one-dimensional collapse of a tube [9,10]. It can be shown that for $\tau_c = 1$ the tube is completely collapsed under the influence of the surface tension alone ($\Delta p = 0$) from infinitly large initial radii to $r_i = 0$. Practically, the tube is mostly collapsed by a moved heating zone and the value of $\tau_c$ can be calculated substituting dt by $dz/v_b$.

$$\tau_c = \frac{\sigma \Delta z_b}{2\eta\, v_b\, (r_a^2 - r_i^2)^{1/2}} \qquad (12)$$

where $v_b$ is the velocity and $\Delta z_b$ is the axial width of the heating zone. Note that for varying temperature the viscosity becomes a function of the axial position and must be considered by integration of $1/\eta$ over dz. Then, $\eta$ in (12) is the viscosity at the maximum of the axial temperature profile, and $\Delta z_b$ is an effective profile width which can be estimated by methods derived in [11]. For a certain pressure difference, the tube diameter remains constant. This „equilibrium pressure" $p_{eq}$ can be used for the determination of the surface tension, see section 3.

$$\Delta p_{eq} = \sigma(r_a^{-1} + r_i^{-1}) \qquad (13)$$

#### 2.3 Application to capillary drawing

In the drawing process,a preform tube is moved into the heating zone of a furnace and is drawn to a fiber capillary by applying a drawing force in the order of 1 N. Consider a volume element $\pi(r_a^2 - r_i^2)\Delta\lambda$ which is moved through the heating zone and is enlarged and partially collapsed. Assuming $v_z$ as constant over the cross section , this process can obviously be described by the equations (5,6,7), if we identify the tube length $\lambda$ with the volume element $\Delta\lambda$. Here, it is advantageous to introduce a dimensionless time according to

$$d\tau_d = \frac{F}{3\pi\, \eta\, (r_a^2 - r_i^2)}\, dt \qquad (14)$$

with

$$K_{1d} = 1 - \frac{\pi\sigma}{F}\, (r_a + r_i) \qquad (15)$$

and

$$K_{2d} = \frac{3\pi\, r_a^2\, r_i^2}{2F}\, (\Delta p - \sigma[r_a^{-1} + r_i^{-1}]) \qquad (16)$$

thus we can replace the corresponding quantities in (5 .. 9).
Stationary relations supposed, the length of the volume element is directly proportional to the axial velocity v in the drawing process, which is $v_p$ (preform feed rate) at the entrance into the heating zone and $v_f$ (fiber drawing velocity) at the exit, so that we can directly replace $\lambda$ in (5) by v. Moreover, we consider that the product $v\,(r_a^2 - r_i^2) = v_p\,(r_{ap}^2 - r_{ip}^2)$ remains constant ($r_{ap}$, $r_{ip}$ are the radii of the starting preform). Hence it follows by integration

$$\tau_d = \frac{F\, \Delta z_b}{3\pi\, \eta\, v_p\, (r_{ap}^2 - r_{ip}^2)} \qquad (17)$$

If $\eta$ varies with z, instead of $\Delta z_b/\eta$ the integral over $dz/\eta$ must be used.
The meaning of $\tau_d$ becomes clear if we neglect for the moment the term $\pi\sigma(r_a + r_i)/F$ compared with 1, satisfied in good approximation for usual drawing conditions. Then we find

$$[1/v]\, dv/d\tau_d = -\, [1/(r_a^2 - r_i^2)]\, d(r_a^2 - dr_i^2)/\, d\tau_d = 1 \qquad (18)$$

$$\tau_d = \ln v_f - \ln v_p \qquad (19)$$

which shows the exponential increase of v and the exponential decrease of the tube cross section area with $\tau_d$.
Further it can be shown on the basis of (18,19), that the „equilibrium pressure" for the tube drawing process, where the ratio of outer and inner radius remains constant, can be described in good approximation by

$$\Delta p_{eq} \approx 2\sigma(r_{ap}^{-1} + r_{ip}^{-1}) \qquad (20)$$

which is just twice the value derived for the case of collapsing (13).

### 3. Surface tension of silica determined by collapsing experiments

Considering (13), the surface tension can be determined very easily by collapsing experiments from the equilibrium pressure where the diameters of the tube remain constant. As already reported in [11], the surface tension of silica in the high temperature region between 1600 and 2000°C is of the order of 0.4 $N \cdot m^{-1}$. Careful experiments with silica tubes of different geometries and different materials (both synthetic silica and quarz glass made by melting of rock crystals in a flame or by electric melting of raw materials) have confirmed the earlier results, some examples are given in Fig.2. For Vycor glass, a remarkable decrease of σ was found and - in contrast to silica - a temperature dependence in form of an increase of σ with rising temperature. In comparison with earlier reported values of 0.28 .. 0.31 $N \cdot m^{-1}$ [12,13], determined by sessile-drop and fiber elongation methods, the collapsing experiments yield distinctly higher values. Unfortunately, in [12,13] the type and the purity of the used glass were not specified in detail. As shown by the comparison with Vycor, already a relatively small change of the silica composition can lead to a pronounced decrease of the surface tension.

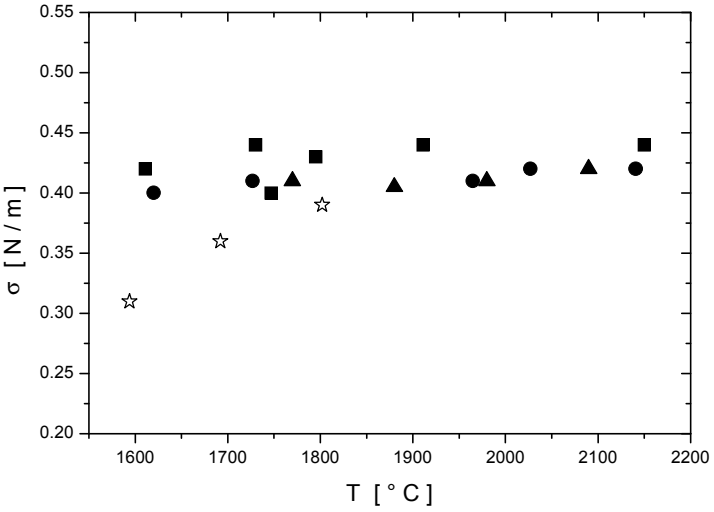


Fig.2 : Surface tension of high silica glasses (experimental error ± 0.02 N/m)

■
● synthetic silica, < 1 ppm OH
▲ synthetic silica, 1200 ppm OH
natural silica, 5 ppm OH
Γ Vycor

### 4. The role of internal pressure in capillary drawing

In the drawing of hollow capillaries from tubes we have also a certain collapsing effect which leads to an increase of the ratio $(r_a-r_i)/r_i$ of the hollow fiber relative to the starting tube, if the pressure difference holds to zero. With increasing Δp, this partial collapse can be diminished, and, the fiber can be blown up even until the fiber is destroyed during drawing.

In Fig.3 and 4, the experimental determined diameter of drawn fibers and the relative wall thickness $(r_a-r_i)/r_i$ for starting tubes 12.5 mm x 9.5 mm and 3 mm x 2 mm, respectively, are compared with the results of the calculations. During a single experimental run, the preform feed rate, the drawing velocity, the temperature and the drawing force were held constant and the inner pressure was varied in secrete temporal steps which are long enough to ensure the achievement of stationary conditions. In general, we find a sufficient agreement between experimental results and calculations. The equilibrium pressure where the tube is neither collapsed nor blown up was found to be about 130 Pa for the tube 12.5 x 9.5 mm and 620 Pa for the tube 3 x 2 mm, respectively, which is also in good agreement with the approximation given by (20).

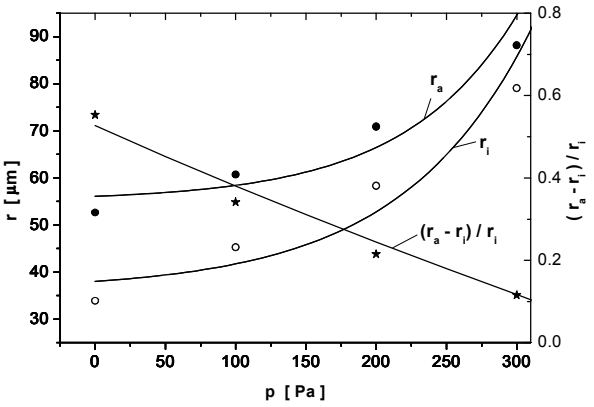


Fig. 3: Hollow fiber dimension- experimental results in comparison with calculations (solid lines) $r_{ap}$: 12.50 mm, $r_{ip}$: 9.50 mm, $v_p$: 0.5 mm/min, $v_f$: 19.8 m/min, F: 0.38 N

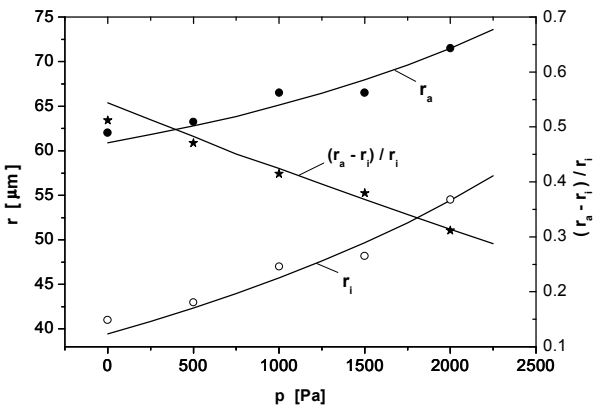


Fig. 4: Hollow fiber dimension- experimental results in comparison with calculations (solid lines) $r_{ap}$: 3.00 mm, $r_{ip}$: 2.05 mm, $v_p$: 0.3 mm/min, $v_f$: 6.7 m/min, F: 0.30 N

## 5. Conclusions

It was shown that the development of capillary dimensions during the collapsing and drawing of silica tubes could be sufficiently well desribed by an elementary model of the viscous flow process. In the preparation of photonic crystal fibers, capillaries with very different but defined dimensions can be fabricated using the effects of surface tension, pressure difference and drawing tension.

---


[1] J. C. Knight, T. A. Birks, P. S. Russel: *Holey Silica Fibers* in V. A. Martel, T. F. George: *Optics of Nanostructured Materials*, John Wiley & Sons, 2001.

[2] F. T. Geyling, Bell Syst. Tech. J. **55**, 1011, 1976.

[3] U. C. Paek, R. B. Runk, J. Appl. Phys. **49**,4417,1978.

[4] P. Gospodinov, A. L. Yarin, Int. J. Multiphase Flow **23**, 967, 1997.

[5] S. D. Sarboh, S. A. Milinkovic, D. L. J. Debeljkovic, Glass Technol. **39**, 53, 1998.

[6] A. D. Fitt, K. Furusawa, T. M. Monro, C. P. Please, J. Lightwave Technol. **19**, 1924, 2001.

[7] G. W. Scherer, J. Am. Ceram. Soc. **60**, 236, 1977.

[8] A. Sommerfeld in *Mechanik der deformierbaren Medien*, Akademische Verlagsgesellschaft Geest & Portig K.-G., Leipzig 1970.

[9] J. A. Lewis, J. Fluid Mech. **81**, 129, 1977.

[10] J. Kirchhof, phys. stat. sol. (a)**60**, K127, 1980.

[11] J. Kirchhof, Cryst. Res. Technol. **20**, 705, 1985.

[12] N. M. Parikh, J. Am. Ceram. Soc. **41**, 18, 1958.

[13] W. D. Kingery, J. Am. Ceram. Soc. **42**, 6,1959.